Petrology, Vol. 10, No. 1, 2002, pp. 23–38. Translated from Petrologiya, Vol. 10, No. 1, 2002, pp. 30–45.
Original Russian Text Copyright © 2002 by Lobanov, Kazansky, Kuznetsov, Zharikov, Nikitin, Ivankina, Zamyatina.
English Translation Copyright © 2002 by MAIK "Nauka/Interperiodica" (Russia).

Correlation of Archean Rocks from the Kola Superdeep Borehole and Their Analogues from the Surface: Evidence from Structural–Petrological, Petrophysical, and Neutron Diffraction Data

K. V. Lobanov*, V. I. Kazansky*, A. V. Kuznetsov*, A. V. Zharikov*, A. N. Nikitin, T. I. Ivankina**, and N. V. Zamyatina****

** Institute of the Geology of Ore Deposits, Petrography, Mineralogy, and Geochemistry, Russian Academy of Sciences, Staromonetnyi per. 35, Moscow, 109017 Russia*
e-mail: Lobanov@igem.ru

*** Frank Laboratory of Neutron Physics, Joint Institute for Nuclear Research, Dubna, Moscow oblast, 141980 Russia*
Received April 5, 2001

Abstract—The paper reports the results of complex studies of core samples of Archean rocks from the Kola Superdeep Borehole and analogues of these rocks collected at the surface. The analogy of these rocks is justified by the determined quantitative proportions of minerals, their microprobe analyses, and analysis of mineral assemblages using microstructural, petrophysical, and neutron diffraction methods. Particular attention is focused on the anisotropy of the rocks and its description based on a variety of techniques. Consequently, the first petrological, structural, and petrophysical characteristics are obtained for the framework that composes deep-seated zones of the ancient continental crust and in which later processes could proceed. The paper is the first to present the results of complex analysis of different types of information on the three-dimensional geological space. The first data are also reported on the changes in the porosity and permeability of the rocks composing the core when it is recovered from significant depths.

INTRODUCTION

The drilling of the Kola Superdeep Borehole (SG-3) was performed with the aim to solve a wide spectrum of geological and geophysical problems, including obtaining as full as possible information on the composition and physical state of rocks and geologic processes at great depths, elucidating the nature of geophysical boundaries in the continental Earth's crust, and modernizing techniques employed in the analysis of rocks and ores in deep-seated crustal zones (*Kol'skaya sverkhglubokaya*, 1984).

While some of these problems were unambiguously solved, others remain a matter of research and discussion until nowadays. Correlations of Archean rocks recovered by the Kola Superdeep Borehole and collected at the surface remains a challenging problem. The point is that the borehole penetrated, within the depth interval of 0–6.8 km, the Early Proterozoic Pechenga Complex, whose stratigraphy is very fully represented by core samples and can be unambiguously correlated with data obtained at the surface, from exploration boreholes, and in mines. The study of rocks of the Archean Kola Series, which was penetrated by Borehole SG-3 in the interval of 6.8–12.2 km, turned to be a more difficult problem. The difficulties are related to the disking of the core recovered from great depths and to the uncertainty of the nature of the anomalously low acoustic wave velocities and high porosity of Archean rocks in core samples lifted from depths below 8 km.

The problems became even more burning after the approval of a new project within the frames of the International Geological Correlation Program, namely, IGCP Project 408, "Rocks and Minerals at Great Depths and on the Surface" (Mitrofanov and Gorbatsevich, 1998).

This paper presents the first results of joint works conducted by specialized research teams at the Institute of the Geology of Ore Deposits, Petrography, Mineralogy, and Geochemistry (IGEM), Russian Academy of Sciences, and the Joint Institute for Nuclear Research (JINR), on the complex study of reference samples of Archean rocks from the core of Borehole SG-3 and their analogues from the Mustatunturi locality at the surface. The researches carried out at IGEM were based on the deep geodynamical model for the Pechenga ore district, collection of reference samples of rocks from the core and their analogues at the surface, and the structural–petrological and petrophysical study of all of these samples. The research team of JINR conducted neutron diffraction analysis of the reference samples of rocks and their analogues and obtained their characteristics that cannot be determined by conventional geological techniques.

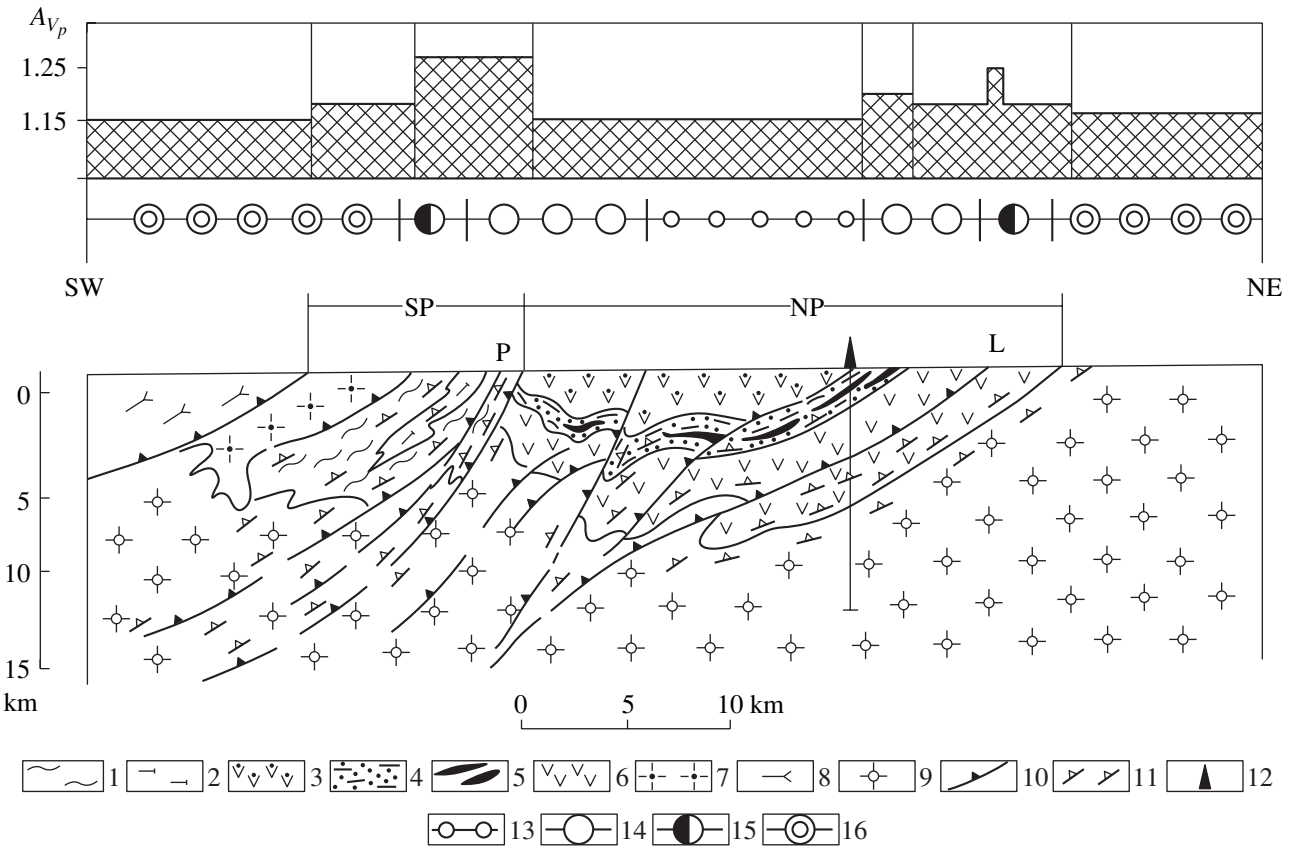

Fig. 1. Integrated 3D geodynamic model of the Pechenga ore district.

(1–2) South Pechenga Series: (1) metabasalts and schists, (2) metaandesites; (3–6) North Pechenga Series: (3) metavolcanics of the Pilgujarvi Formation, (4) metasediments of the productive member, (5) Ni-bearing mafic–ultramafic intrusions, (6) metavolcanics and metasediments of the Kolasiioki, Kuetsjarvi, and Almalahti formations; (7) Proterozoic reomoprhic granitoids; (8) gneisses and schists of the Tundra Series; (9) Archean gneisses, migmatites, and amphibolites of the Kola Series; (10) faults; (11) schistose crystalline rocks; (12) Kola Superdeep Borehole; (13–16) metamorphic facies: (13) prehnite–pumpellyite, (14) greenschist, (15) epidote amphibolite, (16) amphibolite. SP is the southern limb of the Pechenga structure, NP is the northern limb of the Pechenga structure, L is the Luchmompol' fault, P is the Por'itash fault; A_{V_p} is the coefficient of 3D anisotropy of the velocities of longitudinal waves.

SELECTION OF REFERENCE CORE SAMPLES AND THEIR ANALOGUES AT THE SURFACE

The integrated 3D geodynamic model of the Pechenga ore district was developed by formalizing and correlating the Borehole SG-3 section and a 100-km-long surface reference profile across the entire Pechenga district, from the Allarechka ore field in the southwest to the Mustantunturi Range in the northeast. The profile also crossed the Early Proterozoic Pechenga structure, in whose northern limb the Kola Superdeep Borehole is situated (Kazansky *et al.*, 1994). According to this model, the Early Proterozoic sedimentary–volcanic complex was deposited on a stable Archean basement and then underwent extensive reversed faulting, overthrusting, and prograde zonal metamorphism, with these processes also affecting the older rocks of the Kola Series (Fig. 1).

The Pb/Pb zircon age of the protolith of the Kola Series sampled from the core of Borehole SG-3 was estimated at 2.9 Ga, and its metamorphism was dated at 2.0–1.8 Ga (*Arkheiskii kompleks…*, 1991). The Kola Series is dominated by gneisses and includes bodies of amphibolites and metamorphosed ultramafic rocks. The gneisses are mostly biotite–plagioclase, biotite–amphibole–plagioclase in composition. Some units contain high-Al minerals, such as andalusite, garnet, and staurolite. The mineral assemblages and the compositions of coexisting minerals from rocks of the Kola Series point to the amphibolite facies metamorphism. Up to the borehole bottom, the Archean complex includes zones of cataclasis and retrograde metamorphism of the greenschist facies. It was determined that both the cataclasis and the retrograde metamorphism of the Archean rocks were associated with changes in rock densities, porosities, and acoustic properties. Because of this, the first criterion in the selection of reference samples of the Archean rocks was the absence (or very insignificant grades) of retrograde alterations.

The second criterion is related to the necessity to exclude the effect of intensive disking of the core at

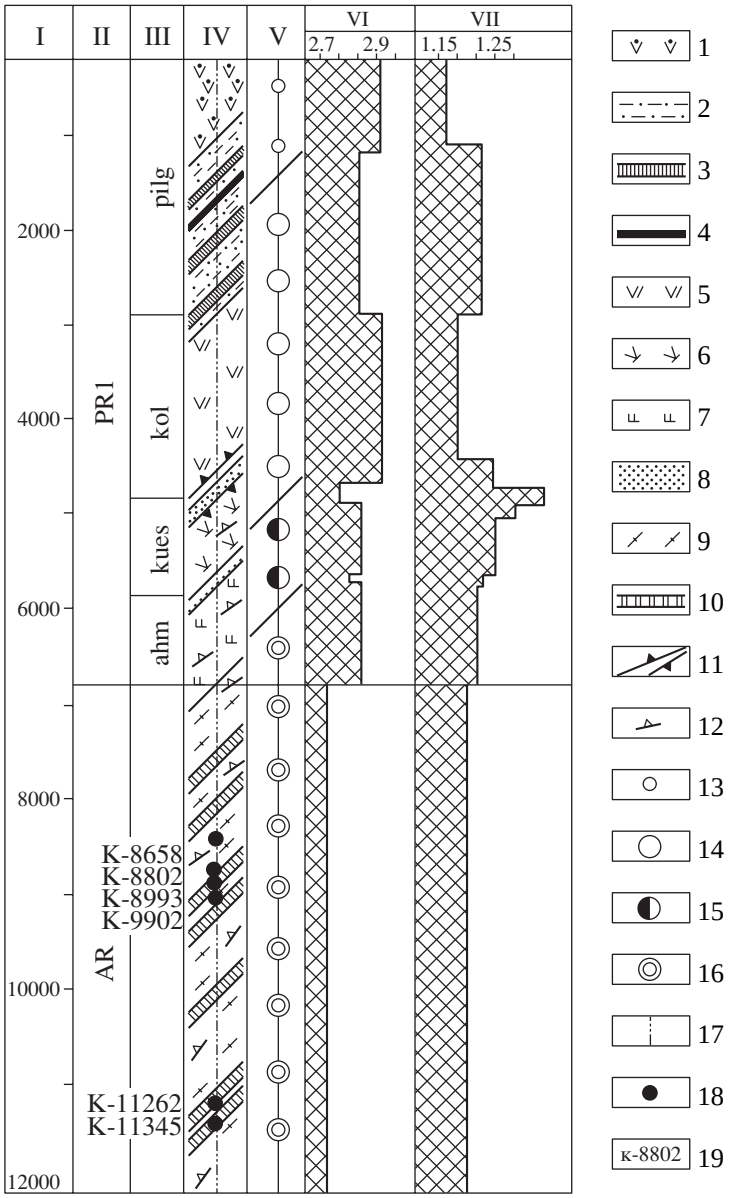

Fig. 2. The Kola Superdeep Borehole section.

(I) Depth, m, (II) age, (III) formations of the North Pechenga Series: pilg—Pilgujarvi, kol—Kolosioki, kues—Kuessjarvi, ahm—Ahmalahti; (IV) rocks; (V) metamorphic facies; (VI) density, g/cm^3; (VII) coefficient of the 3D anisotropy of longitudinal wave velocities.

(1) Metabasalts and picrites; (2) metasediments of the productive member; (3) mafic intrusions; (4) Ni-bearing mafic–ultramafic intrusions; (5) metabasalts; (6) metabasalts and metatrachybasalts; (7) metamorphosed andesites and basaltic andesites; (8) metasedimentary rocks; (9) gneisses and migmatites; (10) amphibolites (not to scale); (11) Luchmompol' fault; (12) crystalline schistose rocks; (13–16) metamorphic facies: (13) prehnite–pumpellyite, (14) greenschist, (15) epidote-amphibolite, (16) amphibolite; (17) borehole axis; (18) sampling sites of Archean rocks; (19) sample numbers (K-8658, K-8802, and K-9002 are gneisses, K-8933, K-11263, and K-11345 are amphibolites).

great depths when the drilling is conducted with the use of standard roller cutters. Core disks of usual thicknesses of 1 to 3 cm are most strongly affected by technogenic factors and, thus, are little suitable for laboratory determination of their physical properties. However, even at great depths, small intervals were drilled by diamond bits. The core from these intervals consists of intact cylinders 6 cm in diameter and 30–40 cm long, with a clear top–bottom orientation. These cylinders were used to prepare reference samples, from which plates were cut for petrographic examinations and 4-cm cubes for neutron diffraction studies.

Finally, the third criterion is the grain sizes of the rocks. The biotite–amphibole gneisses, gneisses with

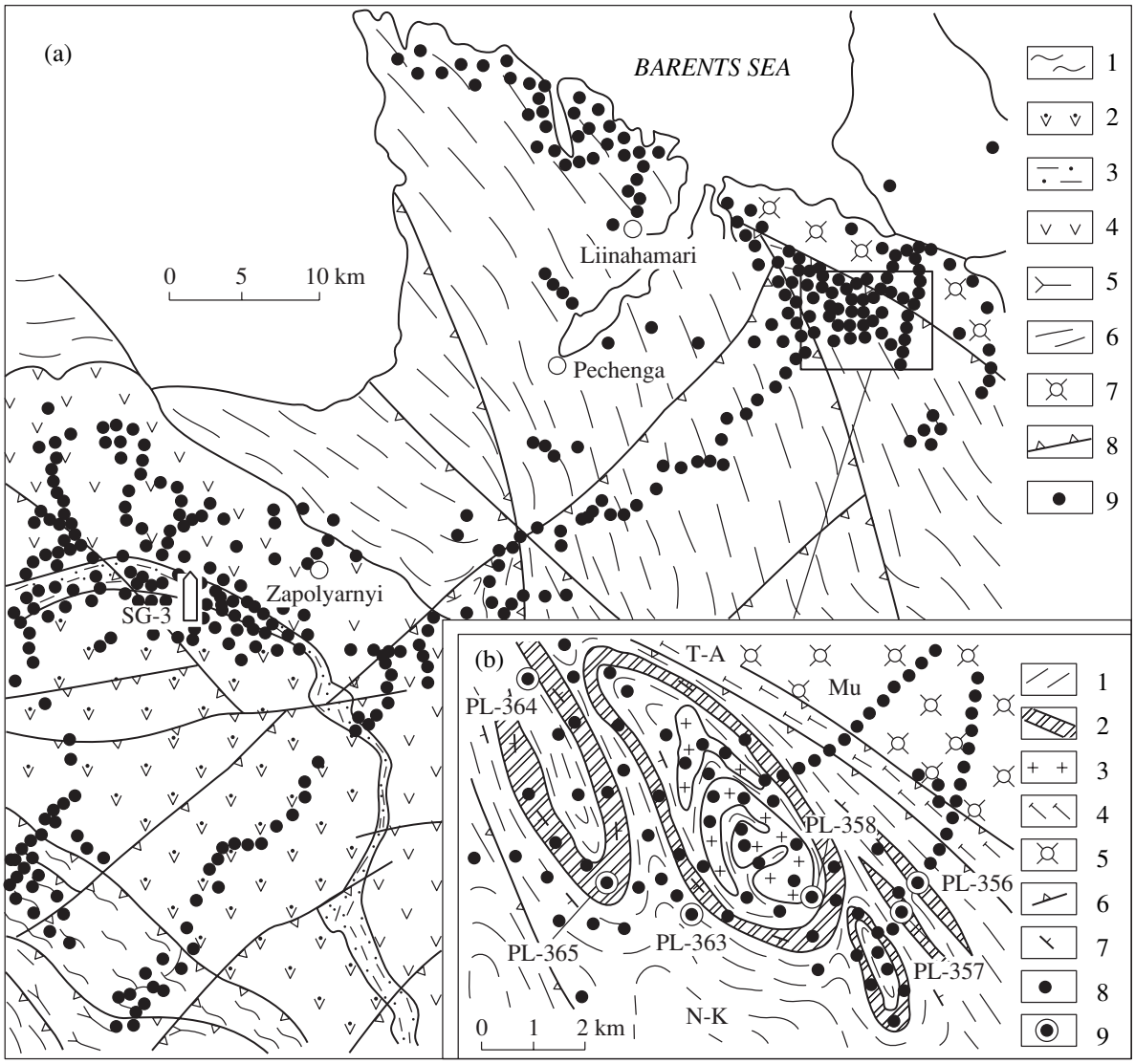

Fig. 3. Schematic map of surface sampling sites in (a) the Pechenga ore district and (b) the Mustatunturi reference area.

(a) (1) South Pechenga Series (metabasalts, schists, and metaandesites); (2–4) North Pechenga Series: (2) metavolcanics of the Pilgujarvi Formation, (3) metasediments of the productive unit, (4) metavolcanics and metasediments of the Kolasiyoki, Kuetsjarvi, and Almalahti formations; (5) gneisses and schists of the Tundra Series; (6) Archean gneisses, migmatites, and amphibolites of the Kola group; (7) Archean granite-gneisses, granites, and enderbites of the Murmansk block; (8) faults; (9) sites from which oriented samples were taken. SG-3 is the Kola Superdeep Borehole.

(b) (1–2) Kola Series: (1) biotite–plagioclase gneisses, (2) amphibole–biotite–plagioclase gneisses and amphibolites; (3) plagiogranites; (4) blastomylonites and blastocataclasites; (5) granite-gneisses, granites, and enderbites; (6) faults; (7) strikes and dips of rocks; (8) sites from which oriented samples were taken and (9) sites from which oriented samples were taken and the numbers of the samples (PL-358, PL-363, and PL-364 are gneisses, PL-358 PL-356, PL-357, and PL-365 are amphibolites). Mu is the Murmansk block, T-A is the Titovsko–Ambarnyi fault, N-K is the Norway–Kola block.

high-Al minerals, and metaultramafics are usually coarse-grained and schistose or have augen structures. Because of this, preference was given to more homogeneous, fine-grained biotite–plagioclase and two-mica gneisses, migmatites, and amphibolites, which are the most widespread in the Borehole SG-3 section.

Of the rocks recovered by the Kola Superdeep Borehole, we selected three samples of biotite–muscovite–plagioclase gneisses (K-8658, K-8802, and K-9002) and three samples of amphibolites (K-8933, K-11262, and K-11345) (Fig. 2). Numbers after the K letter correspond to the depths of sampling.

As can be seen from the comparison of Figs. 1 and 2, the metamorphic zoning in the succession penetrated by Borehole SG-3 is compatible with the zoning observed at the surface in the Pechenga structure and

neighboring Archean rocks north of it. In selecting possible sites for sampling rock analogues, we employed a complex of geologic–structural and petrographic criteria (Lobanov *et al.*, 1999). Because of some technical problems in the Kola Superdeep Borehole, a number of strings was drilled below a depth of 7 km. This made it possible to determine that, at depths of 8–12 km, the Kola Series composes dome-shaped and lineal folds that are cut by faults.

Correspondingly, at the surface, we selected the Mustatunturi site at a distance of 45 km northeast of the borehole because of similarities between the geologic structures. The site consists of Kola Series rocks, which are metamorphosed to the amphibolite facies and the least altered by cataclasis and retrograde metamorphism (Fig. 3). At the Mustatunturi site, rocks of the Kola Series are folded into dome-shaped anticlines and narrow synclines from 3 to 9 km, striking 340° NW. The rocks are biotite–plagioclase gneisses and migmatites developed after these rocks, with beds of biotite–amphibole–plagioclase gneisses and amphibolites. The inner portions of these dome-shaped structures are made up of migmatites and plagiogranites.

Initially, we took 120 samples of metamorphic rocks of the Kola Series at the Mustatunturi site for petrographic and petrophysical examination. Of them, we selected 11 samples with textural features and mineral compositions similar to those of core samples from the Kola Borehole. These samples represent biotite–plagioclase gneisses (PL-358, PL-363, and PL-364), amphibolites (PL-356, PL-357, and PL-365), and migmatites.

By the present, we completed the structural–petrological and petrophysical study of 12 samples of gneisses and amphibolites from the Kola Superdeep Borehole and analogous rocks from the Mustatunturi site and the neutron diffraction analysis of six of these samples.

STRUCTURAL–PETROLOGICAL STUDY

Our structural–petrological examination of the core of the Borehole SG-3 was based on specialized documentation of borehole section and involved studying the structures and textures of rocks, analyzing their mineral assemblages, determining the composition of the minerals on a microprobe, and identifying the spatial orientation of quartz, carbonate, chlorite, mica, and hornblende grains using microstructural techniques (Kazansky, 1987). Our study was centered, first of all, on identifying the relations between metamorphism and deformations in rocks at different depth levels.

Our results establish the coevality of overthrusting and zonal metamorphism in rocks of the North Pechenga and Kola groups and allowed identification of four metamorphic facies in the section penetrated by the Borehole SG-3: prehnite–pumpellyite (0–1400 m), greenschist (1400–4900 m), epidote-amphibolite (4900–6000 m), and amphibolite (>6000 m) (Fig. 2). We also determined that the amphibolite facies extends from the North Pechenga into the Kola Series up to the maximum depth penetrated by the borehole (Fig. 2). Moreover, it was established that massive and bedded structures give way to crystalline schistose ones with depth, with the latter resulting from ductile deformations. The sharp transition between the two structural styles coincides with the zone of the Luchmompol' fault, the first inclined seismic discontinuity (Glagolev *et al.*, 1987).

The results of our petrographic and mineralogical examination of reference samples of the Archean gneisses and amphibolites from Borehole SD-2 and their analogues samples at the surface are summarized in Tables 1–3. These results are in agreement with data on the mineral assemblages of rocks and the chemistry of metamorphic minerals from the depth intervals in the Borehole SG-3 from which the samples were taken. All of the samples display finely schistose structures and lepidogranoblastic textures with equilibrium relations between the metamorphic minerals. The amphibolites typically contain assemblages of high-Al hornblende with plagioclase of oligoclase-andesine to andesine composition (*An* 31–38), while the gneisses usually bear assemblages of biotite with more sodic plagioclase (mainly, *An* 20–23). All biotite gneisses contain muscovite, but its concentrations in rocks recovered from the borehole is higher (4–7 vol %). The causes of this phenomenon are not fully clear, and, conceivably, the occurrence of muscovite in biotite–plagioclase gneisses is controlled by migmatization of rocks of the Kola Series.

The microstructural analysis of gneisses and amphibolites of the Kola Series from the Borehole SG-3 demonstrates that all of these rocks have granoblastic structures (Figs. 4, 5). In a vertical section parallel to the core axis and perpendicular to the schistosity, the optic axes of quartz grains define a belt in the periphery of the projection. Biotite flakes mostly lie in the schistosity plane, and prismatic hornblende grains are elongated in a horizontal direction, i.e., parallel to the axis of the R tectonite after quartz. The samples of Archean rocks taken from the surface exhibit the same structures and analogous orientations of quartz, biotite, and hornblende grains.

The mineral assemblages of the rocks and the compositions of coexisting equilibrium minerals in them (taking into account experimental data) suggest that metamorphism and associated deformations of the Kola Series rocks penetrated by Borehole SG-3 proceeded at temperatures of 550–650°C and pressures of no more than 0.3–0.4 GPa (Glagolev *et al.*, 1987). The same limits are typical of the metamorphic temperatures of the amphibolites from the borehole and their analogues from the surface (data of the plagioclase–hornblende geothermometer; Perchuk and Ryabchikov, 1976; Table 4).

Table 1. Mineralogical composition (vol %) of Archean rocks from the Kola Superdeep Borehole (SG-3) and from the surface at the Mustatunturi site

Rock group	Sampling locality	Sample no.	Minerals							
			Pl	*Hbl*	*Bt*	*Qtz*	*Ms*	*Kfs*	*Grt*	*Ap, Spn, Ep, Car*
Gneisses	Borehole SG-3	K-8568	54		7	31	4			4
		K-8802	59		7	26	5			3
		K-9002	55		9	26	7			3
	Surface	PL-358	48		20	27	1		1	2
		PL-363	50		21	26	1			2
		PL-364	47		18	26	1	5		3
Amphibolites	Borehole SG-3	K-8933	23	63	1	11				1
		K-11262	22	70	2	4				2
		K-11345	24	68	2	3				3
	Surface	PL-356	26	65	3	4				2
		PL-357	21	67	3	7				2
		PL-365	20	70	4	3				3

Note: Here and below, the following mineral symbols are used: *Pl* = plagioclase, *Hbl* = hornblende, *Bt* = biotite, *Qtz* = quartz, *Ms* = muscovite, *Kfs* = K–Na feldspar, *Grt* = garnet, *Ap* = apatite, *Spn* = sphene, *Ep* = epidote, and *Car* = carbonates.

PETROPHYSICAL STUDY

The study of the orientation of metamorphic minerals with microstructural techniques revealed the same deformation patterns in the North Pechenga and Kola series during the Proterozoic zonal metamorphism. At the same time, we met with certain limitations of these techniques in application to studying of quartz-free metabasites and estimating the intensity of deformations coeval with zonal metamorphism. These difficulties were bypassed by constructing diagrams of the anisotropy of longitudinal waves by the methods developed by V.I. Starostin (1979). In essence, the technique involves (1) sounding of two mutually perpendicular plane-parallel plates cut out of a core section or oriented samples and (2) computer-based construction of 3D V_p diagrams. The study of Precambrian metamorphic rocks in the Chupa–Louhi area have demonstrated that their anisotropy belongs to a specific petrostructural–deformational type (Lobanov *et al.*, 1982) and does not depend on the primary lithology of the rocks. Later on, it was determined that diagrams of V_p anisotropy reflect the overall orientation of all rock-forming minerals, i.e., are more informative than microstructural diagrams, with the most representative parameter being the coefficient of the 3D anisotropy of longitudinal waves, A_{V_p}. The latter was calculated from 74 individual measurements in a given sample as a ratio of the area of the maximum longitudinal ultrasonic velocities to the velocity in the minimal area (Kazansky *et al.*, 1985).

During our laboratory investigation, we determined, in addition to elastic characteristics, the open porosity of the rocks. Variations in the density and A_{V_p} in the section of the Kola Superdeep Borehole are portrayed in Fig. 2.

The results of examination of reference samples of the Archean gneisses and amphibolites from the Kola Superdeep Borehole and their analogues from the surface at the Mustatunturi site are summarized in Table 5 and shown in Figs. 4 and 5. They demonstrated the differences between the physical properties of the rocks.

The average density of gneisses and amphibolites from Borehole SG-3 is only 1–2% lower than the analogous characteristics of rocks from the surface, while the velocities of the longitudinal waves in the former are much lower (5.57 and 5.83 km/s, 6.29 and 6.50 km/s, respectively). The average values of open porosity of gneiss samples from the core are 1.12%, and the analogous values for the samples from the surface are 0.61%; these values for the amphibolites are 0.97 and 0.60%, respectively. The diagrams of the anisotropy of longitudinal waves for samples from the core and from the surface exhibit similar configurations: the maximum V_p values group in the schistosity plane or near it, i.e., are controlled by the structural pattern of the rocks. At the same time, the 3D anisotropy coefficient of longitudinal waves is apparently higher in the core samples than in their analogues from the surface.

Table 2. Composition of minerals (wt %) from gneisses from the Kola Superdeep Borehole and from the surface at the Mustatunturi site

Component	K-8658			K-8802			K-9902			PL-358			PL-363			PL-364		
	Pl	*Bt*	*Ms*	*Pl*	*Bt*	*Ms*	*Pl*	*Bt*	*Ms*	*Pl*	*Bt*	*Ms*	*Pl*	*Bt*	*Ms*	*Pl*	*Bt*	*Kfs*
SiO_2	63.86	33.79	46.88	63.86	33.79	47.67	67.35	35.25	46.14	61.54	39.06	49.19	62.24	38.08	41.00	63.78	37.63	65.59
TiO_2	0.02	3.38	0.59	0.02	3.38	0.65	–	2.72	0.38	–	3.04	0.10	–	2.92	–	–	3.27	–
Al_2O_3	21.79	16.88	28.40	21.79	16.88	30.31	20.75	16.40	30.77	23.80	18.82	37.61	23.74	19.08	26.60	24.36	18.24	19,46
FeO	0.07	22.16	3.78	–	22.16	4.53	–	25.09	3.06	–	14.00	0.91	–	12.44	6.20	–	14.73	–
MnO	–	0.36	0.03	0.07	0.36	0.04	–	–	–	–	0.01	–	–	–	–	–	–	–
MgO	–	9.08	2.36	0.04	9.07	2.33	–	5.78	0.99	–	13.76	0.44	–	12.44	6.61	–	13.88	–
CaO	3.94	0.12	0.06	1.68	0.12	0.09	0.91	0.07	0.06	4.32	–	0.03	4.45	–	0.05	4.60	0.07	0.36
Na_2O	8.72	0.42	0.22	10.41	0.42	0.28	10.33	0.12	0.19	9.31	0.18	1.00	10.09	0.06	0.13	9.04	0.15	2.64
K_2O	0.12	9.70	10.46	0.12	9.70	11.01	0.15	9.71	10.68	0.25	10.07	8.93	0.29	10.35	9.72	0.27	9.92	13.46
Total	98.52	95.89	92.78	97.99	95.88	96.91	99.49	95.31	92.27	99.22	98.94	98.21	100.81	95.37	90.31	102.05	97.89	101.51
Si	2.86	2.63	3.19	2.86	2.63	3.19	3.02	2.78	3.19	2.73	2.72	3.13	2.71	3.02	3.00	2.77	2.75	2.96
Al(IV)	1.15	1.37	0.81	1.15	1.37	0.81	1.06	1.22	0.81	1.25	1.28	0.87	1.22	0.98	1.00	1.24	1.25	1.03
Al(VI)	–	0.18	1.60	–	0.18	1.58	–	0.30	1.70	–	0.27	1.95	–	0.80	1.29	–	0.32	–
Ti	–	0.20	0.03	–	0.20	0.03	–	0.16	0.04	–	0.16	–	–	0.18	–	–	0.18	–
Fe	–	1.44	0.22	–	1.44	0.25	–	1.65	0.17	–	0.82	0.05	–	0.82	0.38	–	0.79	–
Mn	–	0.02	–	–	0.02	–	–	0.01	–	–	–	–	–	–	–	–	–	–
Mg	–	1.05	0.25	–	1.05	0.23	–	0.68	0.10	–	1.64	0.04	–	1.47	0.72	–	1.51	–
Ca	0.19	0.01	–	0.08	0.01	0.01	0.04	0.01	0.01	0.21	–	–	0.21	–	–	0.21	–	0.01
Na	0.75	0.07	0.03	0.90	0.07	0.04	0.87	0.02	0.02	0.80	0.03	0.12	0.85	0.01	0.02	0.76	0.02	0.23
K	0.01	0.96	0.93	0.01	0.96	0.94	0.01	0.97	0.95	0.01	0.90	0.72	0.01	1.05	0.90	0.02	0.92	0.77
f	–	0.58	–	–	0.58	–	–	0.71	–	–	0.33	–	–	0.36	–	–	0.34	–
no. *Pl*	20			8			5			21			20			23		

Note: Here and in Table 3. Analyses were conducted by V.A. Boronikhin on a Cameca microprobe at the Institute of the Geology of Ore Deposits, Petrography, Mineralogy, and Geochemistry, Russian Academy of Sciences. *f* = Fe/(Fe + Mn + Mg), dash means not detected.

Table 3. Composition of minerals (wt %) from amphibolites from the Kola Superdeep Borehole and from the surface at the Mustatunturi site

Component	K-8939			K-11262			K-11345			PL-356			PL-357			PL-365		
	Pl	*Hbl*	*Bt*	*Pl*	*Hbl*	*Bt*	*Pl*	*Hbl*	*Bt*	*Pl*	*Hbl*	*Bt*	*Pl*	*Hbl*	*Bt*	*Pl*	*Hbl*	*Bt*
SiO_2	59.41	45.28	37.93	62.18	45.22	38.33	58.49	44.75	38.44	60.55	41.74	34.71	57.93	47.20	36.28	59.32	44.28	34.72
TiO_2	–	0.73	1.76	–	1.02	2.37	–	0.30	1.50	–	1.35	4.20	–	0.38	2.11	–	1.05	2.22
Al_2O_3	25.47	10.05	17.66	25.36	11.59	17.39	27.74	17.39	17.24	23.81	12.21	15.79	27.31	9.15	17.49	26.12	12.06	17.22
FeO	–	17.05	18.39	–	19.65	17.77	–	14.52	14.30	–	22.55	25.59	0.12	14.33	18.72	–	19.54	20.08
MnO	–	0.32	0.22	–	0.27	0.17	–	0.09	0.00	–	0.35	0.24	–	0.29	0.22	–	0.33	0.19
MgO	–	11.20	11.96	–	8.21	10.98	–	8.79	13.93	–	6.65	9.64	0.09	12.63	11.14	–	8.48	10.09
CaO	7.05	11.87	0.33	5.64	11.16	0.04	8.19	11.05	–	5.73	11.37	0.58	8.17	12.80	0.34	7.21	11.42	0.46
Na_2O	6.93	1.49	0.46	8.74	2.12	0.15	7.27	2.17	0.31	7.13	1.69	0.41	8.08	1.22	0.08	8.21	2.10	–
K_2O	0.41	0.93	9.09	0.12	1.04	9.87	0.05	0.30	9.21	0.23	1.15	8.67	0.11	0.51	9.59	0.05	0.86	9.78
Total	99.27	98.92	97.80	102.04	100.28	97.07	101.74	99.36	94.93	97.45	99.06	99.83	101.81	98.51	95.97	100.91	100.12	94.76
Si	2.67	6.70	–	2.70	6.64	2.83	2.56	6.43	2.85	2.82	6.37	2.68	2.53	6.91	2.74	2.61	6.55	–
Al(IV)	1.36	1.30	–	1.30	1.33	1.17	1.44	1.67	1.15	1.27	1.63	1.32	1.41	1.09	1.26	1.35	1.45	–
Al(VI)	–	0.45	–	–	0.68	1.10	–	1.27	0.35	–	0.56	0.04	–	0.48	0.30	–	0.61	–
Ti	–	0.08	–	–	0.12	0.14	–	0.03	0.89	–	0.16	0.25	–	0.04	0.12	–	0.12	–
Fe	–	2.11	–	–	2.42	0.10	–	1.74	0.89	–	2.68	1.67	–	1.75	1.18	–	2.42	–
Mn	–	0.04	–	–	0.04	0.01	–	0.01	0.01	–	0.05	0.02	–	0.04	0.01	–	0.04	–
Mg	–	2.47	–	–	1.81	1.21	–	1.88	1.54	–	1.51	0.89	–	2.75	1.25	–	1.87	–
Ca	0.34	1.88	–	0.26	1.76	–	0.38	1.70	–	0.28	1.96	0.05	0.38	2.00	0.03	0.34	1.81	–
Na	0.61	0.43	–	0.74	0.60	0.02	0.62	0.60	0.04	0.62	0.50	0.06	0.68	0.34	0.01	0.70	0.60	–
K	0.02	0.18	–	0.01	0.20	0.93	–	0.05	0.87	0.01	0.22	0.86	–	0.10	0.53	–	0.16	–
f	–	0.47	–	–	0.58	0.48	–	0.48	0.37	–	0.66	0.67	–	0.28	0.48	0.57	–	–
no. *Pl*	35			26			38			31			36			33		

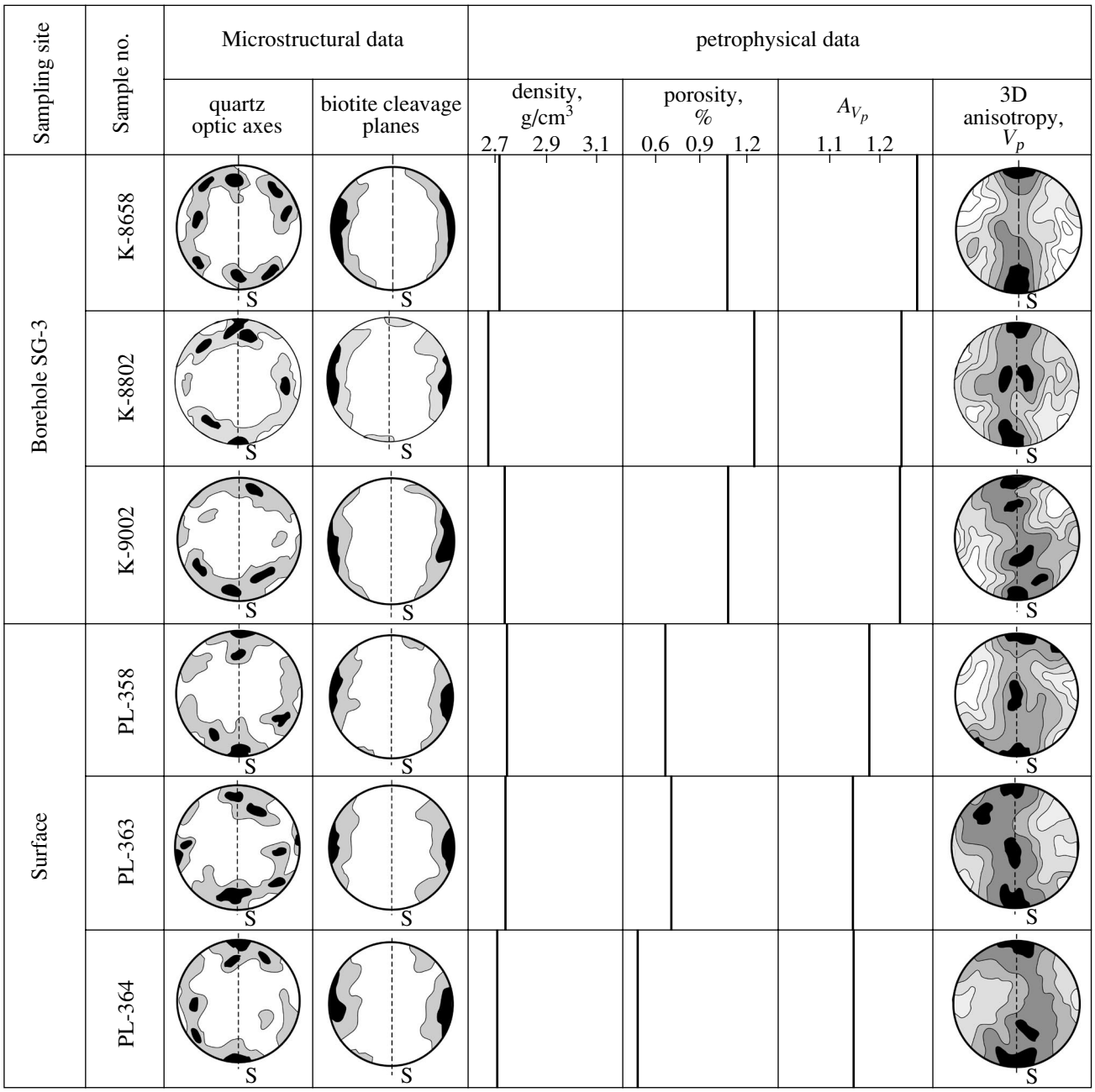

Fig. 4. Microstructural diagrams for the orientation of minerals and petrophysical diagrams for the V_p 3D anisotropy of gneiss samples from the Borehole SG-3 and from the surface.

All diagrams are projections onto a vertical plane perpendicular to the schistosity; S is the schistosity, A_{V_p} is the coefficient of V_p 3D anisotropy.

This pertains to both gneisses and amphibolites (1.23–1.25 and 1.14–1.16, respectively).

TEXTURE MEASUREMENTS BY NEUTRON DIFFRACTION

The quantitative structural analysis was conducted at the pulsed reactor IBR-2 of the Frank Laboratory of Neutron Physics of the Joint Institute for Nuclear Research by the time-of-flight neutron diffraction. The theoretical fundamentals of the technique were described by Aksenov and Balagurov (1996). On passing through a moderator, neutrons from a pulsed reactor move along a neutron guide to the sample, are scattered on it, and recorded by a SKAT diffractometer. Due to the high penetration of neutrons into matter, this technique makes it possible to investigate the structures of

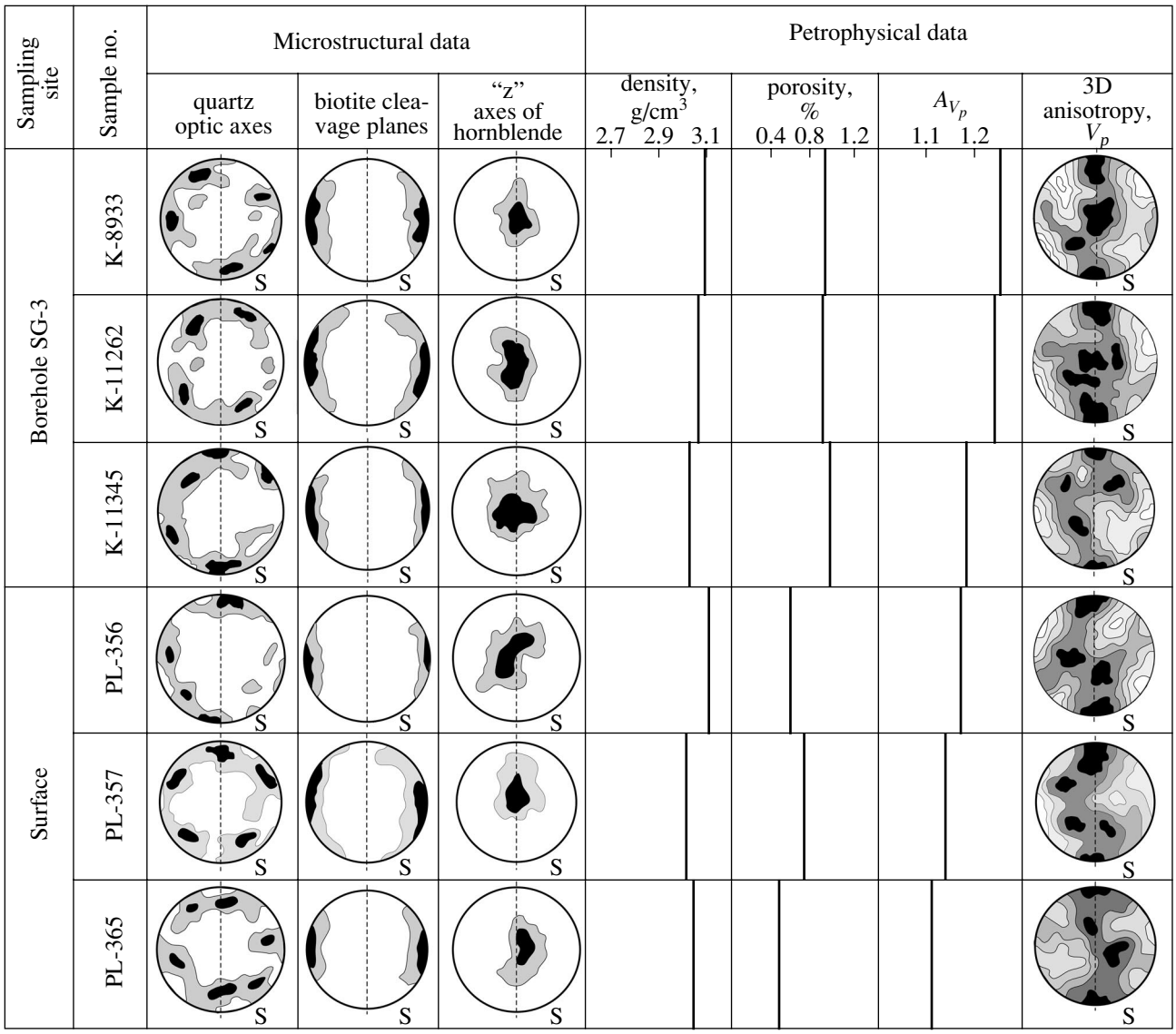

Fig. 5. Microstructural diagrams for the orientation of minerals and petrophysical diagrams for the V_p 3D anisotropy of amphibolite samples from the Borehole SG-3 and from the surface.

All diagrams are projections onto a vertical plane perpendicular to the schistosity; S is the schistosity, A_{V_p} is the coefficient of V_p 3D anisotropy.

large rock samples (up to 50 by 50 by 50 mm) throughout their volumes.

In contrast to pole figures (PF), which reflect the spatial distribution of specific crystallographic directions (*hkl*), the orientation distribution function (ODF) describes the preferred crystallographic structure of the whole volume of the sample. The reliability of the obtained ODF can be confirmed by comparing theoretical PF calculated based on ODF with experimentally measured ones in the same crystallographic direction (*hkl*).

The ODF were reconstructed for the predominant minerals of core samples and their surface analogues of the Kola Series. Based on the orientation distribution functions, the pole figures of the main crystallographic planes of quartz and plagioclase in the gneiss samples, as well as the main crystallographic planes of hornblende and plagioclase in the amphibolite samples, were recalculated (Figs. 6, 7).

The texture analysis of biotite plagiogneisses from the core of Borehole SG-3 (Samples K-8658 and K-9002) and their analogues from the surface (Samples (PL-358 and PL-363) led us to the following conclusions. The degree of preferred orientation of the samples (i.e., the volume fraction of mineral grains oriented in a certain direction) is weaker for quartz than for plagioclase, whereas the structural sharpness (i.e., the maximum pole density in the pole figures) of these min-

Table 4. Metamorphic temperatures of amphibolites (calculated by the plagioclase–hornblende thermometer)

Sample no.	Ca = Ca/(K + Na + Ca)		Temperature, °C
	Pl	*Hbl*	
Core samples			
K-8933	0.35	0.76	580
K-11262	0.26	0.69	570
K-11345	0.38	0.73	630
Analogous rocks from the surface			
PL-356	0.32	0.76	550
PL-357	0.36	0.82	580
PL-365	0.33	0.70	620

erals are roughly equal. At the same time, the preferred orientation of plagioclase from Samples K-9002 and PL-358 exhibits patterns of a higher symmetry than the preferred orientation of quartz.

From the comparison of the (001), (010), and (100) basal plane plagioclase figures in the core samples (K-8933 and K-9002) with their surface analogues (PL-358 and PL-363; Fig. 6), it is obvious that the preferred orientation patterns of all samples are similar in terms of the symmetry and configuration of the contour lines.

The texture analysis of amphibolite samples from the core (K-8933, K-11262, and K-11345) and their surface equivalents (PL-356 and PL-365) revealed that the hornblende textures are characterized by a more pronounced predominant orientation than the plagioclase textures.

The hornblende textures of all samples (both lifted from the borehole and taken at the surface) show obvious similarities in the preferential orientation patterns, particularly those of the (100), (010), and (001) crystallographic planes. The sample analogues from the surface (PL-356 and PL-365) are characterized by a good agreement of the basal pole figures. Practically identical configurations of pole density lines on PF were observed in Samples K-8933 and K-11345 (from the core), PL-356 and PL-365 (from the surface). However, the sharpness of the hornblende texture is higher in samples from the surface than in those from the core

Table 5. Petrophysical characteristics of gneisses and amphibolites from the Kola Superdeep Borehole and from the surface at the Mustatunturi site

Rock group	Sampling locality	Sample no.	ρ	Π	V_p	V_s	μ	G	φ	K	V_p/V_s	A_{V_p}
			g/cm^3	%	km/s	km/s		10^{-4} MPa				
Gneisses	Borehole SG-3	K-8658	2.72	1.07	5.48	2.61	0.34	2.07	5.53	5.68	2.1	1.25
		K-8802	2.68	1.23	5.52	2.68	0.34	2.13	5.68	5.64	2.06	1.25
		K-9002	2.74	1.07	5.72	2.88	0.33	2.4	6.36	6.09	1.99	1.22
		Total	2.71	1.12	5.57	2.72	0.34	2.2	5.86	5.8	2.05	1.24
	Surface	PL-358	2.75	0.74	5.88	3.23	0.28	2.8	7.18	5.44	1.82	1.18
		PL-363	2.75	0.63	5.83	3.13	0.29	2.65	6.84	5.61	1.86	1.15
		PL-364	2.71	0.46	5.79	3.18	0.28	2.69	6.89	5.34	1.82	1.15
		Total	2.74	0.61	5.83	3.18	0.28	2.71	6.97	5.46	1.83	1.16
Amphibolites	Borehole SG-3	K-8933	3.09	0.96	6.32	3.32	0.31	3.34	8.75	7.63	1.9	1.26
		K-11262	3.06	0.94	6.22	3.34	0.3	3.35	8.69	7.13	1.86	1.24
		K-11345	3.03	1	6.34	3.26	0.32	3.17	8.35	7.72	1.94	1.18
		Total	3.06	0.97	6.29	3.31	0.31	3.28	8.6	7.49	1.9	1.23
	Surface	PL-356	3.07	0.6	6.55	3.45	0.31	3.58	9.38	8.2	1.89	1.17
		PL-357	3.02	0.69	6.37	3.42	0.3	3.45	8.95	7.41	1.86	1.14
		PL-365	3.05	0.5	6.59	3.48	0.3	3.62	9.45	8.14	1.89	1.12
		Total	3.05	0.6	6.5	3.45	0.3	3.55	9.26	7.91	1.88	1.14

Note: ρ is the density, Π is the open porosity, V_p and V_s are the velocities of longitudinal and transverse waves, μ is the Poisson coefficient, G is the shear modulus, φ is Young's modulus, K is the bulk modulus, and A_{V_p} is the V_p 3D anisotropy coefficient.

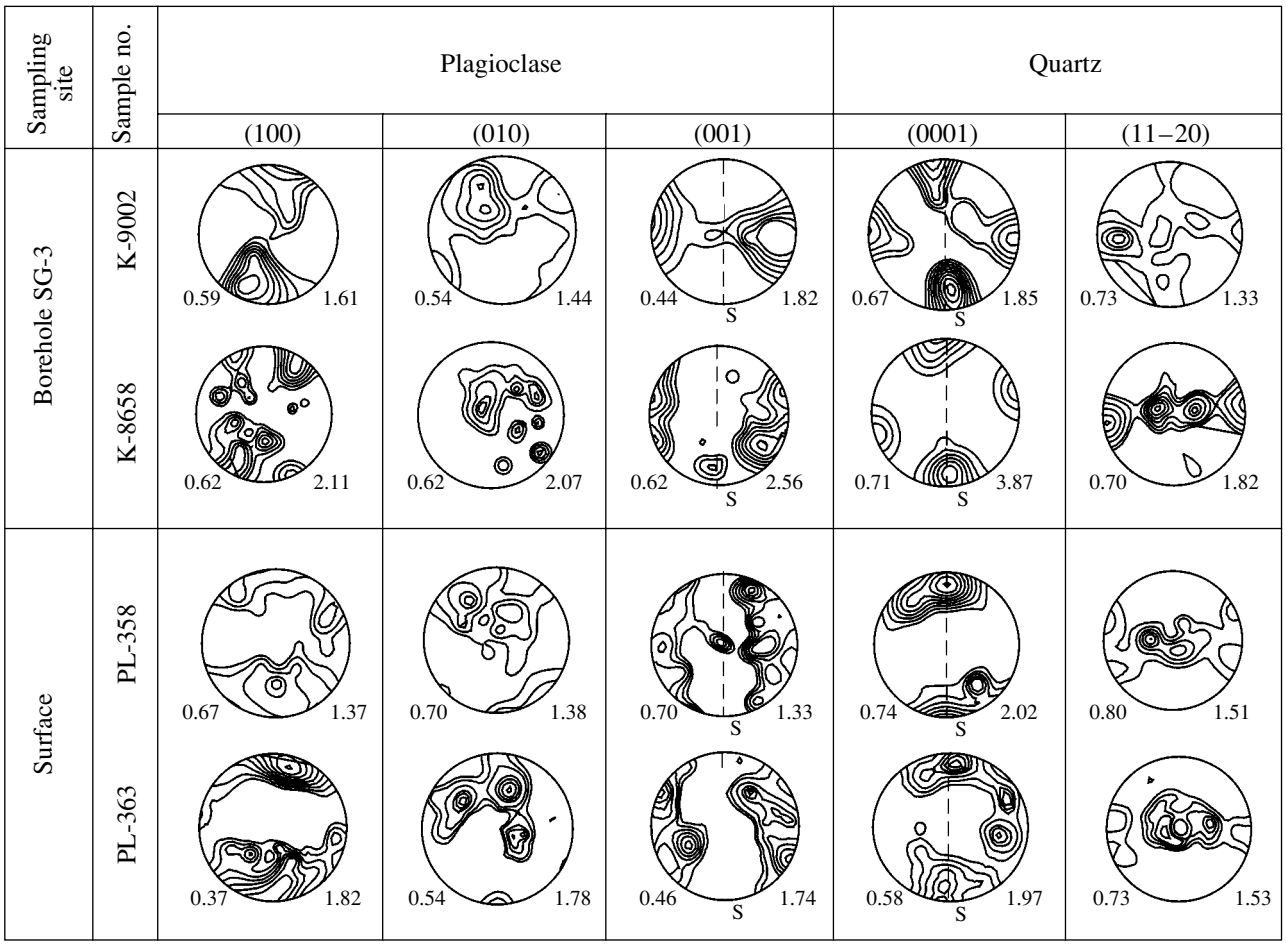

Fig. 6. Pole figures of quartz and plagioclase, based on ODF, for samples from the Borehole SG-3 and from the surface.

(except Sample K-11345). This is also confirmed by the results of quantitative structural analysis.

No differences as significant as those in the hornblende textures were observed in the preferred orientation of plagioclase in core and surface samples. Plagioclases possesses a weaker preferred orientation than hornblende does, except in core sample K-8933, which displays a relatively regular distribution of contour lines.

POROSITY AND PERMEABILITY OF ARCHEAN ROCKS

In the monograph devoted to the Kola Superdeep Borehole (*Kol'skaya sverkhglubokaya…*, 1984), it was mentioned that the anomalously high (1.9–4.9%) open porosity of the Archean rocks at depths below than 7 km is caused by the interaction of drilling equipment with the material at the borehole bottom and a decrease in the core density during its lifting to the surface. These conclusions were confirmed by the comparison of the porosity of rocks at the peripheral and central parts of core samples (Kremenetskii and Ovchinnikov, 1986) and the acoustic polaroscopy (Gorbatsevich and Basalaev, 1993).

The data cited below on the water saturation in the reference core samples of gneisses and amphibolites and their analogues from the surface, as well as the results of experimental studies at high temperatures and pressures, enabled us to quantify the aforementioned phenomena.

The porosity and water saturation parameters of Archean gneisses and amphibolites are listed in Table 6. They were obtained by the technique of free water saturation in rock samples at room temperature and atmospheric pressure. The average porosity of gneisses from the core samples K-8658, K-8802, and K-9002 and from the surface samples PL-358, PL-363, and PL-364 are 1.13 and 0.61%, respectively. The amphibolites exhibit analogous differences: their average porosity in the core is 0.97% (Samples K-8933, K-11262, and K-11345) and 0.6% in surface samples (Samples PL-356, PL-357, and PL-365). The analysis of the expotential water saturation regime from the time of quasi-instantaneous saturation (15 min) to the maximum saturation of rocks indicates that gneiss and amphibolite samples

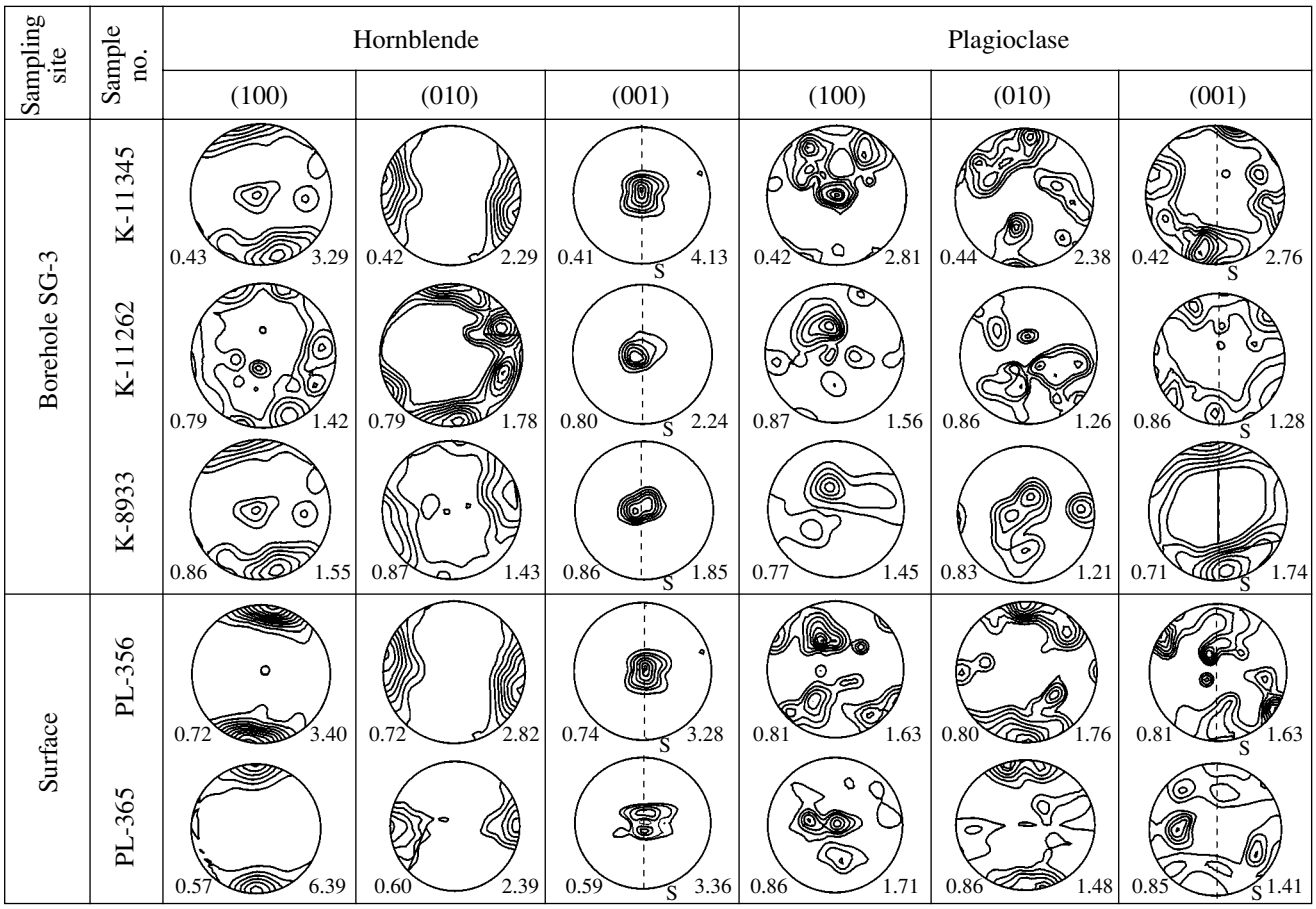

Fig. 7. Pole figures of plagioclase and hornblende, based on ODF, for samples from the Borehole SG-3 and from the surface.

both from Borehole SG-3 and from the surface are characterized by the same values of saturation constant (B), equal to 0.04–0.05. However, the quasi-instantaneous saturation (A) during the first 15 min of laboratory experiment is much higher for the core samples than for the gneisses and amphibolites from the surface: 0.89–0.72 and 0.37–0.44%, respectively. This demonstrates that core samples contain more through-pores and pore conduits of regular configurations and larger diameters than those in samples from the surface. It can be hypothesized that the differences between the open porosity values and water-saturation parameters are caused by the decompaction of core samples during their lifting from great depths to the surface.

The permeability of rocks is one of the main parameters controlling fluid flows in the Earth's crust (Fyfe, 1978). However, the technically induced decompression of the core makes it more difficult to *in situ* assay these values for rocks from the Kola Superdeep Borehole. Because of this, we carried out special experiments (at high temperatures and pressures) of the permeability of the Archean gneisses and amphibolites intersected by the Borehole SG-3.

In these experiments, we used amphibolite (Sample PL-356) taken at the surface and core samples, whose mineral composition and structural features were similar to those of the reference samples from the same depth intervals of Borehole SG-3, which were drilled with diamond drilling bits.

The experiments on determining the permeability of rocks were conducted at temperatures from 20 to 600°C and pressures from 30 to 150 MPa (Zharikov *et al.*, 1990). This enabled us to estimate the permeability of the rocks under conditions similar to those of their natural occurrence and within the temperature boundaries of the amphibolite facies.

Figure 8 displays the dependence of the permeability of the samples from SD-3 core and their analogues from the surface. The dependence was measured at the simultaneous heating and loading of the rocks to imitate an increase in their occurrence depths. The original permeability of core samples ranged from 10^{-17} to 10^{-16} m^2, and the permeability of the analogous rocks from the surface was much lower, approximately 10^{-18} m^2. Comparison of these values demonstrates how strongly technologically-induced decompaction of the core affects the properties of core samples lifted to the sur-

Table 6. Characteristics of the porosity of and water saturation in gneisses and amphibolites from the Kola Superdeep Borehole and from the surface at the Mustatunturi site

Rock group	Sampling locality	Sample no.	ρ	φ	A	T	B	E-time, h			
			g/cm^3	%	%	hours		5	22	69	189
Gneisses	Borehole SG-3	K-8658	2.72	1.07	0.91	24.69	0.04	0.08	0.03	0.02	0.03
		K-8802	2.68	1.23	0.85	18.5	0.04	0.04	0.06	0.04	0.03
		K-9002	2.74	1.09	0.91	14.62	0.05	0.1	0.12	0.04	0.04
		Mean	2.71	1.13	0.89	19.27	0.04	0.07	0.07	0.03	0.03
	Surface	PL-358	2.75	0.74	0.53	13.35	0.05	0.08	0.06	0.04	0.04
		PL-363	2.75	0.63	0.27	14.24	0.05	0.1	0.07	0.04	0.04
		PL-364	2.71	0.46	0.3	17.58	0.04	0.04	0.04	0.06	0.03
		Mean	2.74	0.61	0.37	15.05	0.05	0.07	0.06	0.05	0.04
Amphibolites	Borehole SG-3	K-8933	3.09	0.96	0.74	26.24	0.03	0.03	0.01	0.01	0.03
		K-11262	3.06	0.94	0.61	19.5	0.04	0.06	0.04	0.03	0.04
		K-11345	3.03	1	0.8	14.53	0.05	0.02	0.02	0.08	0.04
		Mean	3.06	0.97	0.72	20.09	0.04	0.04	0.02	0.04	0.04
	Surface	PL-356	3.07	0.6	0.43	16.41	0.05	0.07	0.07	0.06	0.04
		PL-357	3.02	0.69	0.51	19.66	0.03	0.07	0.07	0.02	0.03
		PL-365	3.05	0.5	0.21	19.58	0.04	0.04	0.04	0.04	0.03
		Mean	3.05	0.6	0.44	18.55	0.04	0.06	0.06	0.04	0.03

Note: ρ is the density, φ is the open porosity, A is the quasi-instantaneous saturation, T is the half-saturation time, B is the saturation constant, and E-time is the exponential water saturation regime.

face. With an increase in temperature and pressure to values corresponding to *P–T* parameters of the natural occurrence of Archean rocks in the borehole, this difference decreases. This takes place simultaneously with the overall systematic decrease in the porosity of all of the samples: with approaching the *in-situ P–T* parameters of the deep levels penetrated by Borehole SG-3 (6–10 km), the permeability decreases by one to three orders of magnitude compared with the original values and attains 10^{-21}–10^{-19} m^2 (Fig. 8).

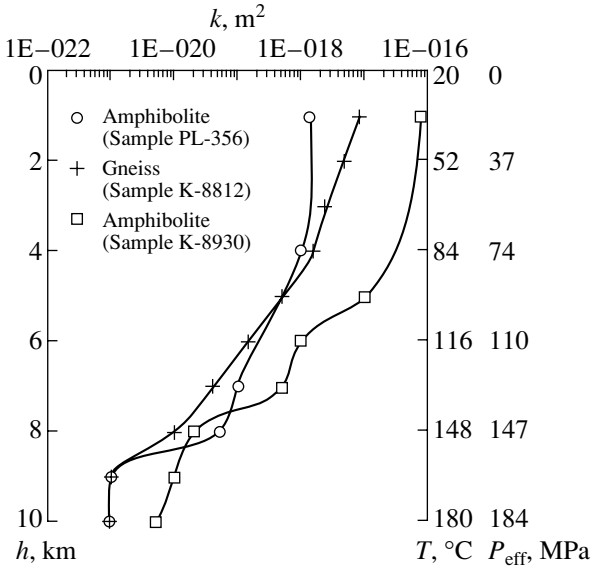

Fig. 8. Correlation of the permeability (*k*) of gneiss and amphibolite samples from the Borehole SG-3 and from the surface with the sampling depth.

At temperatures of the prograde metamorphism in rocks of the Kola Series, the permeability of the samples varies from 10^{-19} to 10^{-17} m^2, while these values at the temperatures of the retrograde metamorphism are much lower, 10^{-21} to 10^{-19} m^2. Hence, the permeability of rocks during prograde metamorphism was high enough for fluid flow to permeate the whole rock volume. These values during retrograde metamorphism were several orders of magnitude lower, so that fluids should have been focused to large structural discontinuities in the rocks, such as faults and tectonic zones.

CONCLUSION

The results of complex structural–petrological, petrophysical, and neutron diffraction studies of core samples from the Kola Superdeep Borehole and analogous rocks from the surface are of principal importance for characterizing the framework in which later processes developed in deep zones of the continental crust.

Earlier, the studies of the Kola Superdeep Borehole led to the conclusion that the metamorphic degree and intensity of deformation and rock anisotropy increase with depth, but these variations are not linear, being controlled by a combination of several factors. Data for the northern limb of the Pechenga structure and its framework are in conflict with these observations, but generally, the anisotropy of longitudinal waves at the surface is lower than at a depth.

At the same time, microstructural and neutron diffraction studies of reference core samples and their analogues from the surface uncovered some unusual characteristics of the anisotropy of the Kola Series rocks, such as the more pronounced preferential orientation of hornblende grains compared with that of plagioclase grains and the latter compared with quartz grains. Judging from the composition of coexisting minerals, these orientations were produced at temperatures of the amphibolite facies. The causes of the differences are still not fully clear, and this calls for additional structural analysis of the rocks.

The data received provide a new insight into the continuously debated problem of the anomalously high porosity of rocks and the anomalously low acoustic velocities at deep levels of the ancient continental crust as related to the nature of seismic boundaries and waveguides. The determined physical characteristics of reference core samples and analogous rocks from the surface indicate that the gneisses and amphibolites at depths of 8–11 km are characterized by normal values of density (2.71–2.74 and 3.05–3.06 g/cm^3, respectively) and the velocities of longitudinal (5.57–5.83 and 6.29–6.50 km/s) and transverse (2.72–3.18 and 3.31–3.45 km/s) waves. The decompression during the extraction of the core to the surface leads to its decompaction. As a result, the rock porosity may increase twice and the permeability simultaneously increase by one order of magnitude. The results of our petrophysical researches suggest that the Archean gneisses and amphibolites have an *in-situ* permeability of the order of 0.5% and permeability from 10^{-20} to 10^{-18} m^2.

Our data make it possible to specify the tasks for further researches. These are, first and foremost, (1) studying the inner structures of faults in the crystalline basement and relationships between ductile and brittle deformations of rocks, (2) investigating the processes of transformation and destruction of anisotropic structures in rocks, and (3) experimental examining the structure of the pore space in rocks at elevated temperatures and pressures.

ACKNOWLEDGMENTS

The authors appreciate the participation of V.S. Lanev and Yu.P. Smirnov (of the Kola Superdeep Research and Production Center) and A.A. Glagolev (Institute of the Geology of Ore Deposits, Petrography, Mineralogy, and Geochemistry, Russian Academy of Sciences) in sampling and preliminary studying reference samples of the Archean rocks from the core of the Kola Superdeep Borehole and their analogues at the surface. V.I. Starostin (Geological Department, Moscow State University) is thanked for assistance in the petrophysical studies of the samples. This study was supported by the Russian Foundation for Basic Research (projects nos. 01-05-64244, 01-05-64294, 01-05-62495, 99-05-65698, and the project Leading Research Schools, no. 00-15-96778) with reference to the aims of the International Geological Correlation Program, Project no. 408.

REFERENCES

Aksenov, V.L. and Balagurov, A.M., The Time-of-Flight Neutron Diffractometry, *Usp. Fiz. Nauk*, vol. 166, no. 9, pp. 955–985.

Arkheiskii kompleks v razreze SG-3 (The Archean Complex in the Geologic Section Penetrated by Hole SD-3), Mitrofanov, F.P., Ed., Apatity: Kol'skii Nauch. Tsentr, 1991.

Fyfe, W.S., Price, N.J., and Tompson, A.B., *Fluids in the Earth's Crust*, Amsterdam: Elsevier, 1978. Translated under the title *Flyuidy v zemnoi kore*, Moscow: Mir, 1981.

Glagolev, A.A., Genkin, A.D., Kazansky, V.I., *et al.*, Study of Endogenic Processes Using Materials of Superdeep Drilling, in *Endogennye rudnye raiony i mestorozhdeniya* (Areas with Endogenic Ore Mineralization and Deposits), Moscow: Nauka, 1987, pp. 129–144.

Gorbatsevich, F.F. and Basalaev, A.A., Determination of Parameters of Paleostresses with the Use of Acoustopolarization Method, *Izv. Ross. Akad. Nauk, Ser. Fiz. Zemli*, 1993, vol. 7, pp. 24–31.

Kazansky, V.I., Boronikhin, V.A., Vanyushin, V.A., *et al.*, Interrelations between Deformations, Metamorphism, and the Petrophysical Properties of Rocks from the Pechenga Ore District, in *Vnutrennee stroenie rudonosnykh dokembriiskikh razlomov* (Inner Structure of Mineralized Precambrian Faults), Moscow: Nauka, 1985, pp. 6–46.

Kazansky, V.I., Kuznetsov, O.L., Kuznetsov, A.V., *et al.*, Deep Structure and Geodynamics of the Pechenga Mining District: A Study of the Kol'skaya Superdeep Hole, *Geol. Rudn. Mestorozhd.*, 1994, vol. 36, no. 6, pp. 500–519.

Kazansky, V.I., Tasks and Methods of the Specialized Study of the Core of Superdeep and Deep Holes in Ore Regions, in *Metody i praktika issledovanii glubinnogo stroeniya nedr* (Practice and Methods for the Study of Deep-Seating Structures), Leningrad: Vses. Geol. Inst., 1987, pp. 114–128.

Kol'skaya sverkhglubokaya (The Kola Superdeep Hole), Moscow: Nedra, 1984.

Kremenetskii, A.A. and Ovchinnikov, L.N., *Geokhimiya glubinnykh porod* (Geochemistry of Deep-Seated Rocks), Moscow: Nauka, 1986.

Lobanov, K.V., Glagolev, A.A., Zharikov, A.V., *et al.*, Comparison of Archean Rocks in the Section Penetrated by the Kola Superdeep Hole and at the Earth's Surface, *Geoinformatika*, 1999, no. 4, pp. 38–50.

Lobanov, K.V., Kazansky, V.I., and Starostin, V.I., Structural and Petrophysical Control of Muscovite Pegmatites from the Chupa–Louhi Area, Northern Karelia, in *Rudonosnye struktury dokembriya* (Precambrian Ore-Bearing Structures), Moscow: Nauka, 1982, pp. 137–165.

Mitrofanov, F.P. and Gorbatsevich, F.F., The Aims and Tasks of IGCP Project No. 408, in *Gomologi porod v Kol'skoi sverkhglubokoi skvazhine i na poverkhnosti* (Homologues of Rocks from the Kola Superdeep Hole at the Earth's Surface), Apatity: Kol'skii Nauch. Tsentr, 1998, pp. 3–8.

Perchuk, L.L. and Ryabchikov, I.D., *Fazovoe sootvetstvie v mineral'nykh sistemakh* (Phase Correspondence in Mineral Systems), Moscow: Nedra, 1976.

Starostin, V.I., *Strukturno-petrofizicheskii analiz endogennykh rudnykh polei* (Structural–Petrophysical Analysis of Endogenic Ore Fields), Moscow: Nedra, 1979.

Zharikov, A.V., Vitovtova, V.M., and Shmonov, V.M., An Experimental Study of the Permeability of Rocks from the Kola Superdeep Hole, *Geol. Rudn. Mestorozhd.*, 1990, no. 6, pp. 79–88.